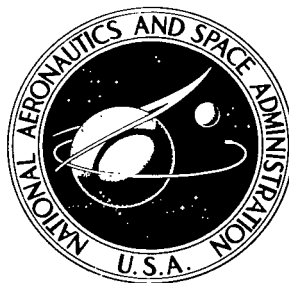


NASA TECHNICAL NOTE



NASA TN D-5224

C.1

LOAN COPY: RETURN TO  
AFWL (WLIL-2)  
KIRTLAND AFB, N MEX

0131976



TECH LIBRARY KAFB, NM

NASA TN D-5224

EXPERIMENTS ON POWER LOSS IN  
HERRINGBONE-GROOVED, GAS-LUBRICATED  
JOURNAL BEARINGS

*by David P. Fleming, Robert E. Cunningham,  
and William J. Anderson*

*Lewis Research Center  
Cleveland, Ohio*



EXPERIMENTS ON POWER LOSS IN HERRINGBONE-GROOVED,  
GAS-LUBRICATED JOURNAL BEARINGS

By David P. Fleming, Robert E. Cunningham, and William J. Anderson

Lewis Research Center  
Cleveland, Ohio

NATIONAL AERONAUTICS AND SPACE ADMINISTRATION

---

For sale by the Clearinghouse for Federal Scientific and Technical Information  
Springfield, Virginia 22151 - CFSTI price \$3.00

## ABSTRACT

Power loss was determined for herringbone journal bearings operating in air to speeds of 60 000 rpm. Power loss (relative to that calculated for a plain bearing of the same dimensions) did not vary widely for the range of geometric variables used. Relative power loss increased with speed and was generally higher than for a plain bearing. The dimensional value of power loss was higher than that in a reference tilting-pad bearing at a speed of 38 500 rpm.

# EXPERIMENTS ON POWER LOSS IN HERRINGBONE-GROOVED, GAS-LUBRICATED JOURNAL BEARINGS

by David P. Fleming, Robert E. Cunningham, and William J. Anderson

Lewis Research Center

## SUMMARY

Experiments were conducted to determine the power loss in herringbone-grooved journal bearings operating in air to speeds of 60 000 rpm. The power loss was calculated from the speed-time plot of the bearing rotor coasting down in speed. Power loss (relative to that calculated for a plain bearing of the same dimensions) did not vary widely for the range of geometric variables investigated. Relative power loss increased with speed and was generally higher than for an equivalent size plain bearing. At a speed of 38 500 rpm, power loss was also greater than that of a reference tilting-pad bearing. Better correlation of the data was obtained using dimensional speed rather than bearing number  $\Lambda$  or Reynolds number.

## INTRODUCTION

Turbomachinery used in space power systems must be compact and lightweight. In addition, since energy sources for these applications are usually limited, internal losses must be minimized. Process fluid lubrication can help to achieve these goals. Components such as oil sumps and pumps, seals, and oil scavenging and separating systems are eliminated. Since the viscosity of the working fluid (usually a gas or liquid metal) is less than that of normal lubricating oils, friction power losses in the bearings can also be reduced. This is especially true when the working fluid is a gas, as in the Brayton cycle machinery currently under development (ref. 1).

Self-excited instability is a severe problem in gas-lubricated bearings; at high speeds and low loads the bearing journal may precess about its steady state position. The frequency of this precession, for a self-acting bearing, is usually about one-half the rotational frequency; thus, the phenomenon has become known as half-frequency whirl. A major part of the research in gas-lubricated bearings has been directed toward devel-

opment of bearing configurations that will operate stably when the load is small or zero.

One design which has operated stably at high speeds, even when unloaded, is the herringbone-grooved bearing (ref. 2). Shallow helical grooves are cut in either the journal or the bearing to create an inward pumping viscous pump. The pressure field created is similar to that in an externally pressurized bearing. In the herringbone bearing, however, the pressure increases continuously with increasing speed.

In order to assure stable operation, clearances in a herringbone bearing must be kept low, approximately  $0.5 \times 10^{-3}$  centimeter radial clearance per centimeter of shaft radius. Thus, power loss in these bearings could well be higher than in other bearing types operating with larger clearances. Because of the nonuniform clearance created by the herringbone grooves, calculation of the friction power loss is not possible with present techniques, and experimental measurements are necessary. In contrast, for a smooth gas journal bearing, friction power loss may be calculated quite easily. Reynolds numbers are almost always low enough so that laminar conditions prevail.

The objectives of this investigation were (1) to measure the friction power loss in herringbone-grooved bearings having various groove angles, widths, and lengths and (2) to compare the power loss with the calculated values for a smooth journal bearing and with available data for other bearing types.

The measurements were made by recording the speed, as a function of time, of a rotor coasting down from high speed. From the speed-time function the acceleration at a given speed was determined; the frictional torque, and hence the power loss, could then be calculated from the rotor moment of inertia. Corrections were made for friction other than that in the herringbone bearings.

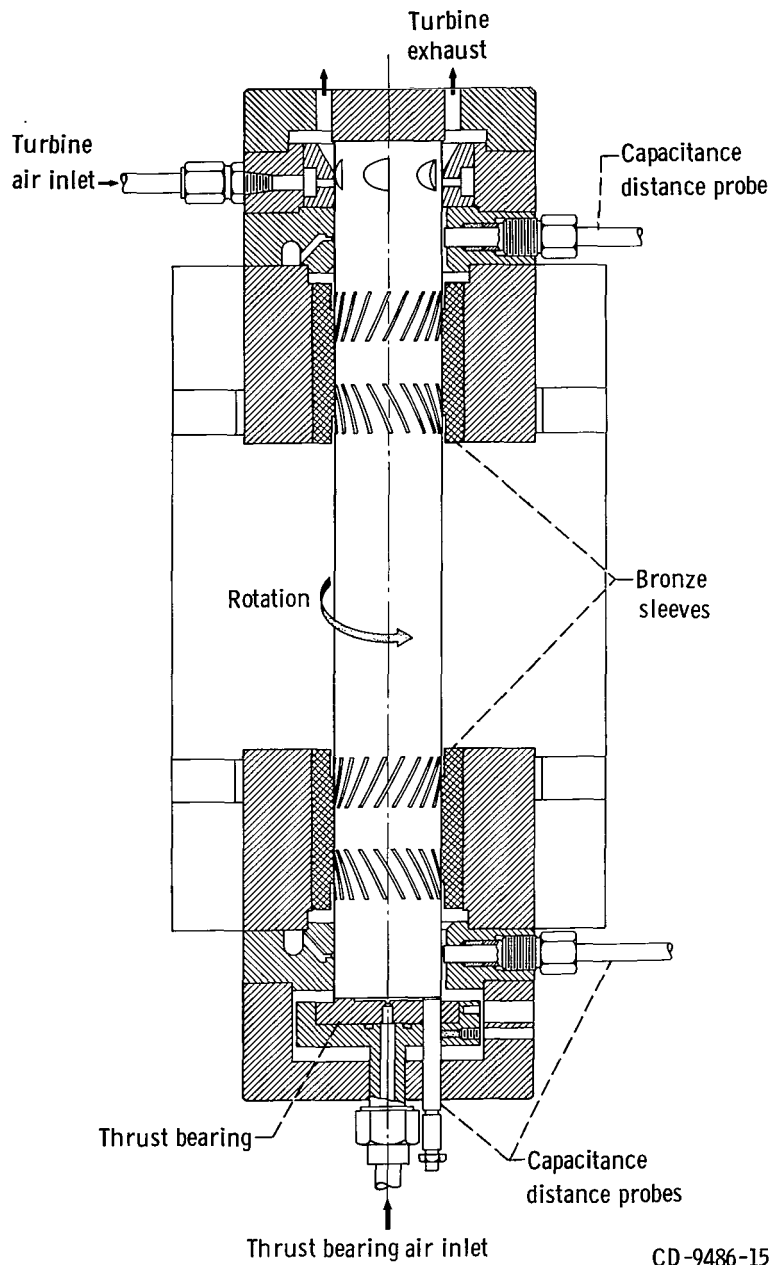
## SYMBOLS

A	coefficient
B	coefficient
C	radial clearance, in.; mm
D	bearing (rotor) diameter, in.; cm
E	elastic modulus, lb/in. <sup>2</sup> ; N/m <sup>2</sup>
H	ratio of groove clearance to ridge clearance
I	rotor polar moment of inertia, (in.)(lb)(sec <sup>2</sup> ); kg m <sup>2</sup>
i	index
J	number of terms in data approximating function

L	bearing length, in. ; cm
L <sub>1</sub>	length of grooves, in. ; cm
N	number of data points
n	number of grooves
P	power loss in herringbone bearing, watts
P <sub>p</sub>	power loss in plain bearing, watts
p	pressure in bearing film, lb/in. <sup>2</sup> ; N/m <sup>2</sup>
p <sub>a</sub>	ambient pressure, lb/in. <sup>2</sup> ; N/m <sup>2</sup>
R	bearing radius, in. ; cm
S	rotor speed, rpm
T	torque, (in.)(lb); (N)(m)
t	time, sec
α	ratio of groove width to width of groove-ridge pair
β	groove angle, degrees
γ	angular extent of bearing, radians
Λ	bearing number, $6\mu\omega R^2/p_a C^2$ , dimensionless
μ	lubricant viscosity, (lb)(sec)/in. <sup>2</sup> ; (N)(sec)/m <sup>2</sup>
ν	Poisson's ratio
ρ	rotor density, (lb)(sec <sup>2</sup> )/in. <sup>4</sup> ; kg/m <sup>3</sup>
σ	rms error of fitted curve, sec
ω	rotor speed, radians/sec

Subscripts:

c	calculated
l	lifter bearing
m	measured
o	zero speed
T	thrust bearing



CD-9486-15

Figure 1. - Test apparatus.

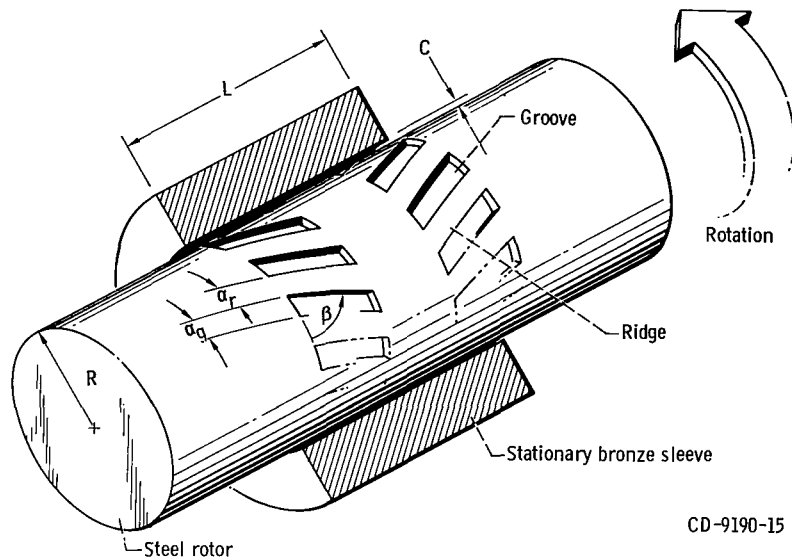


Figure 2. - Herringbone grooved rotor.

## APPARATUS

The experimental apparatus is identical to that used in reference 2 and is described fully therein. It consists of a steel rotor mounted vertically in two smooth bronze bushings which have been in-line bored (fig. 1). The rotor is  $1\frac{1}{2}$  inches (3.8 cm) in diameter and  $12\frac{1}{4}$  inches (31.1 cm) long, and has two herringbone-groove patterns on its surface (fig. 2). Each of the bronze bushings is  $1\frac{1}{2}$  inches (3.8 cm) long; thus, the length to diameter ratio is 1. An externally pressurized thrust bearing supports the rotor at its lower end.

The rotor is driven by an impulse turbine which consists of a number of buckets cut into the upper end of the rotor and a nozzle ring surrounding the rotor. A magnetic pickup adjacent to the turbine buckets is connected to a digital counter to measure rotor speed.

Two orthogonally oriented capacitance distance probes are mounted outboard of each bearing. They were used to measure the assembled clearance of the rotors in the bearings. A fifth capacitance probe, flush with the thrust bearing surface, was used to monitor thrust bearing clearance.

Eight different herringbone-grooved rotors were used with two sets of bronze bearings. The characteristics of the grooves and assembled bearings are listed in table I.

TABLE I. - CHARACTERISTICS OF HERRINGBONE-GROOVED ROTORS

[Groove length to total bearing length ratio, 0.6; rotor weight, 6.06 lb (2.75 kg); rotor length, 12.25 in. (31.1 cm); bearing span, 6.64 in. (16.9 cm); nominal rotor diameter, 1.5 in. (3.8 cm); bearing length to diameter ratio, 1.0.]

Rotor	Groove angle, $\beta$ , deg	Ratio of groove width to width of groove ridge pair, $\alpha$	Number of grooves, n	Groove depth		Zero-speed radial clearance		Ratio of groove clearance to ridge clearance at zero speed, $H_o$	Maximum rotor speed, rpm
				mils	mm	mils	mm		
Low-clearance bronze bushings									
A1	30	0.5	20	0.56	0.014	0.41	0.010	2.4	56 730
A2	35	↓	20	.64	.016	.49	.012	2.3	59 860
A3	35		23	.59	.015	.42	.011	2.4	58 100
A4	40		23	.65	.016	.41	.010	2.6	58 260
A5	40		28	.75	.019	.51	.013	2.5	57 870
A6	35		.3	36	.36	.009	.48	.012	1.8
A7	40	.3	40	.57	.014	.50	.013	2.1	59 750
<sup>a</sup> B1	30	.5	20	.50	.013	.49	.012	2.0	58 700
High-clearance bronze bushings									
A1	30	0.5	20	0.56	0.014	0.56	0.014	2.0	54 200
A2	35	↓	20	.64	.016	.67	.017	2.0	15 980
A3	35		23	.59	.015	.63	.016	1.9	22 830
A4	40		28	.75	.019	.71	.018	2.1	16 180

<sup>a</sup>Fully grooved,  $L_1/L = 1$ .

## PROCEDURE

### Experimental

The procedure for assembly of the apparatus and running up to speed was the same as described in reference 2. After maximum speed was reached, the turbine air was shut off, and the rotor allowed to coast down in speed. During the coast period, readings of the digital speed counter were recorded at regular time intervals. These time intervals were electronically determined by the counter. The length of the interval was subsequently determined by recording the total elapsed time of the experimental run and dividing this time by the number of speed readings. The test was stopped when the rotor speed had decayed to approximately 1000 rpm.

### Data Reduction

With the time interval between speed readings known, a time value could be assigned to each speed reading. These pairs of values defined a speed-time function. The time of the first reading was chosen as zero. The torque acting on the rotor is the product of rotor polar moment of inertia and rotor acceleration.

$$T = -I \frac{d\omega}{dt} \quad (1)$$

The minus sign has been used so that torque will be positive, since acceleration is negative.

The speed-time relation could be numerically differentiated to determine the rotor acceleration. However, numerical differentiation is an inherently inaccurate procedure since small errors in speed or time values can result in proportionately larger errors in acceleration. Rotor acceleration may be determined more accurately by fitting an analytical function to the speed-time relation and differentiating this function analytically. Toward this end, it is convenient to consider time as a function of rotor speed, rather than the usual inverse relation.

For a smooth bearing with constant clearance, the torque acting on the bearing, and hence the acceleration, varies directly with speed.

$$\frac{d\omega}{dt} = \frac{\omega}{A_2} \quad (2)$$

where  $A_2$  is a proportionality constant. Integration of this relation results in

$$t = A_1 + A_2 \ln \omega \quad (3)$$

The function to be fitted to the experimental data was therefore chosen as

$$t = B_1 + B_2 \ln S + B_3 S + B_4 S^2 \quad (4)$$

where  $S$  is the rotor speed in rpm. The terms in  $S$  and  $S^2$  allow for the behavior of the herringbone bearing being different than that of a plain bearing. The coefficients  $B_1$  to  $B_4$  were determined to provide a least-squared-error fit to the particular experimental data being examined.

Differentiation of equation (4) gives

$$\frac{dt}{dS} = \frac{B_2}{S} + B_3 + 2B_4 S \quad (5)$$

From equation (1), the torque acting on the rotor is then

$$T = - \frac{\pi}{30} \frac{I}{\frac{dt}{dS}} \quad (6)$$

and the power loss

$$P = \omega T = - \frac{\pi^2}{900} \frac{I S}{\frac{dt}{dS}} \quad (7)$$

There are power losses in addition to those in the herringbone journal bearings. Two partial arc "lifter" bearings (operated hydrostatically to support the rotor for starting in other types of tests when the rotor is horizontal), the hydrostatic thrust bearing, and general windage all contribute to the power loss. These additional losses must be subtracted from the experimentally measured power loss in order to determine the net loss in the herringbone bearings. Torque, and hence power loss, can easily be calculated

for the lifter and thrust bearings. For one lifter bearing

$$T_l = \frac{\gamma R^3 L \mu \omega}{C_l} \quad (8)$$

where  $\gamma$  is the angular extent of the lifter,  $L$  the length, and  $C_l$  the radial clearance. For the thrust bearing,

$$T_T = \frac{\pi R^4 \mu \omega}{2C_T} \quad (9)$$

Since only a small portion of the rotor is exposed to ambient air, windage losses were neglected.

The entire data reduction process of calculating herringbone clearances from capacitance probe readings, fitting the least-squares curve to speed decay data, and computing torque and power loss values was handled by a digital computer.

## RESULTS AND DISCUSSION

Eight different herringbone-grooved rotors were used in two sets of bronze bearings. Twelve sets of data were recorded (not all of the rotors were run in both sets of bearings). The maximum speed attained was approximately 60 000 rpm. Rotor-bearing characteristics are listed in table I for the configurations tested. The groove depths and clearances listed are averages for the two bearings.

Figure 3 shows a typical set of data points and the least-squares curve fitted. The curve fits the data very well, indicating that the herringbone bearing behaves sufficiently like a plain bearing so that the two correction terms  $B_3S$  and  $B_4S^2$  of equation (4) are sufficient.

A root-mean-square error of the least-squares curve may be defined by

$$\sigma = \left[ \frac{1}{N-J} \sum_{i=1}^N (t_{mi} - t_{ci})^2 \right]^{1/2} \quad (10)$$

where  $N$  is the number of data points,  $J$  is the number of terms in the approximating function (eq. (4)),  $t_{mi}$  is the actual time value corresponding to the  $i$ th data point, and  $t_{ci}$  is the time calculated by equation (4). The divisor has been chosen as  $N - J$

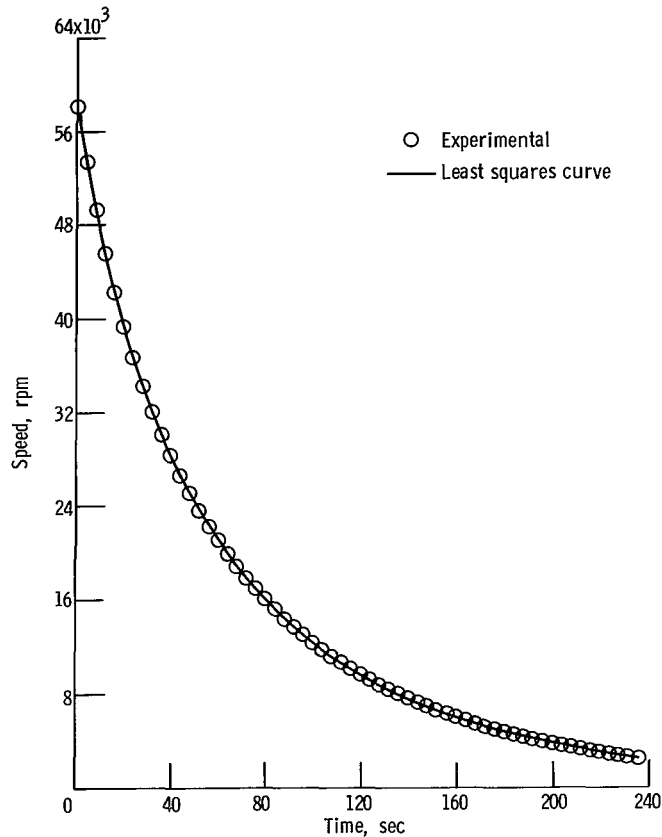


Figure 3. - Speed decay of herringbone-grooved bearing. Rotor A3; clearance, 0.42 mils (0.011 mm).

rather than  $N$  to compensate for the fact that the summation term of equation (10) naturally decreases with increasing  $J$  (if  $J = N$ , the sum would be zero). The factor  $\sigma$  is thus a measure of the smoothness of the data as well as of the fit of the approximating curve. For the tests reported herein,  $\sigma$  varied from 0.021 to 0.24 second. For all but two runs,  $\sigma$  was less than 0.08 second. This may be compared with an average incremental time step of approximately 4 seconds.

Figure 4 shows the variation of torque with speed for the bearing configuration whose speed-time trace appears in figure 3. The upper curve is the gross torque, calculated from equation (6). The lower curve is the net torque due to the two herringbone bearings. It is obtained from the gross torque by subtracting the torque of the lifter and thrust bearings (eqs. (8) and (9)). The pertinent dimensions of the lifter bearings for equation (8) are

- (a)  $\gamma = \pi$  radians
- (b)  $L = 7/8$  in. (22 mm)
- (c)  $C_l = 0.002$  in. (0.05 mm)

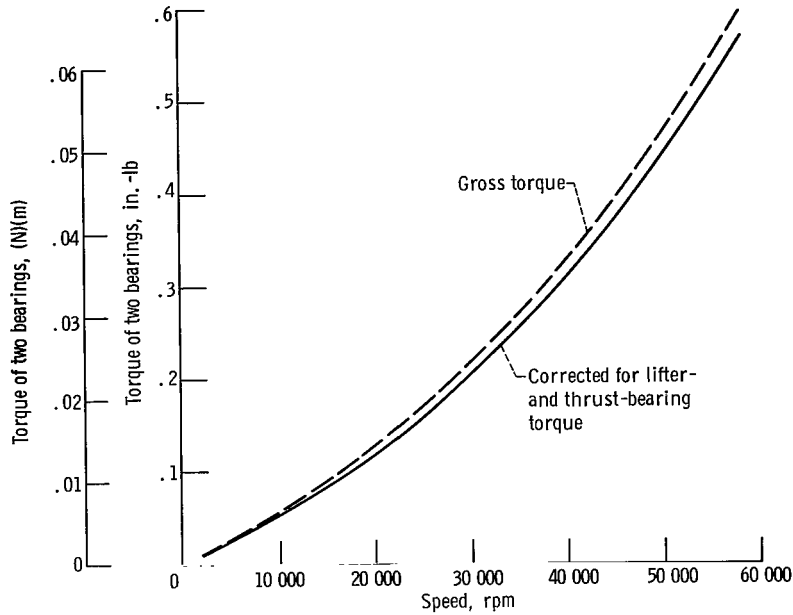


Figure 4. - Torque of herringbone-grooved bearings. Rotor A3; clearance, 0.42 mils (0.011 mm).

The thrust bearing clearance  $C_T$  was usually about 0.001 inch (0.02 mm). The radius of the lifter and thrust bearings is the same as that of the rotor,  $1\frac{1}{2}$  inches (3.8 cm). The correction required to the gross torque is relatively small.

Power loss is calculated as the product of torque and speed (eq. (7)). The solid curve of figure 5 illustrates the power loss as a function of speed for a typical herringbone-grooved bearing; the values were computed from the net torque information appearing in figure 4. Equation (8), which was used to calculate the torque of the lifter bearings, also applies to a full circular journal bearing. If the torque is converted to power by multiplying by the speed, there results

$$P_p = \frac{2\pi\mu\omega^2 R^3 L}{C} \quad (11)$$

where  $\gamma = 2\pi$  for a full circular bearing.

This formula was used to calculate the power loss in a plain bearing having the same dimensions and clearance as the herringbone bearing of figure 5. The result appears as the long-dashed curve of figure 5 (because a plain bearing is inherently unstable, it was not possible to measure its power loss experimentally). The bearing clearance at zero speed was used in this calculation. Because of centrifugal force, the rotor diameter increases with increasing speed; thus the bearing clearance decreases. The increase in

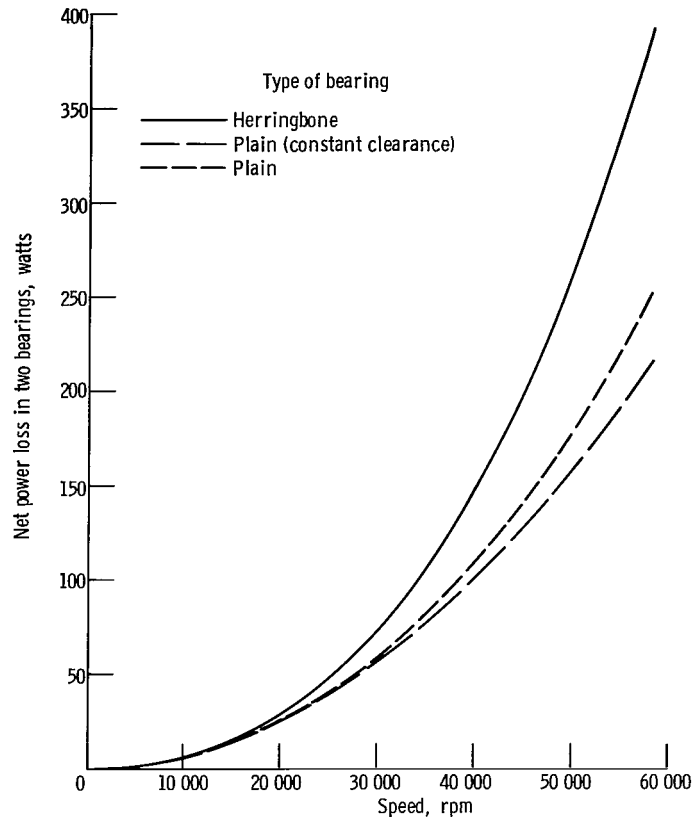


Figure 5. - Power loss of journal bearings. Rotor A3; clearance, 0.42 mils (0.011 mm).

diameter for a solid rotor may be calculated by (ref. 3)

$$\Delta D = \frac{\rho \omega^2 R^3 (1-\nu)}{2E} \quad (12)$$

where  $\nu$  is Poisson's ratio for the rotor,  $\rho$  the rotor density, and  $E$  the elastic modulus. The short-dashed curve of figure 5 shows the power loss of a plain bearing when the decrease in clearance is taken into account.

From equation (11) it is seen that power loss in a plain journal bearing depends inversely on clearance. A comparison of power losses for different herringbone bearings would have little meaning, therefore, unless they could be normalized with respect to clearance. A convenient normalizing function is the power loss in a plain bearing which has the same dimensions and clearance as the herringbone bearing under study. The power loss relative to a plain bearing should not be looked at as a measure of the advantage or disadvantage of using a herringbone bearing rather than a plain bearing. At

medium and high compressibility numbers (above approximately 10), the load capacity of a herringbone bearing is higher than that of a similar size plain bearing (ref. 4). Thus, for a given application a smaller herringbone bearing could be used, with an accompanying smaller power loss. Of course, a plain bearing usually cannot be used at all because of its inherent instability.

The relative power loss  $P/P_p$  has been plotted against speed in figure 6 ( $P$  is the herringbone bearing power loss, and  $P_p$  the power loss in an equivalent plain bearing calculated by eq. (11)). Figure 6(b) is an enlarged plot of the lower speed part of figure 6(a). The rotor designation and zero speed clearance are indicated on each curve. The plain bearing power loss was calculated with a clearance which was corrected for centrifugal growth of the rotor (eq. (12)).

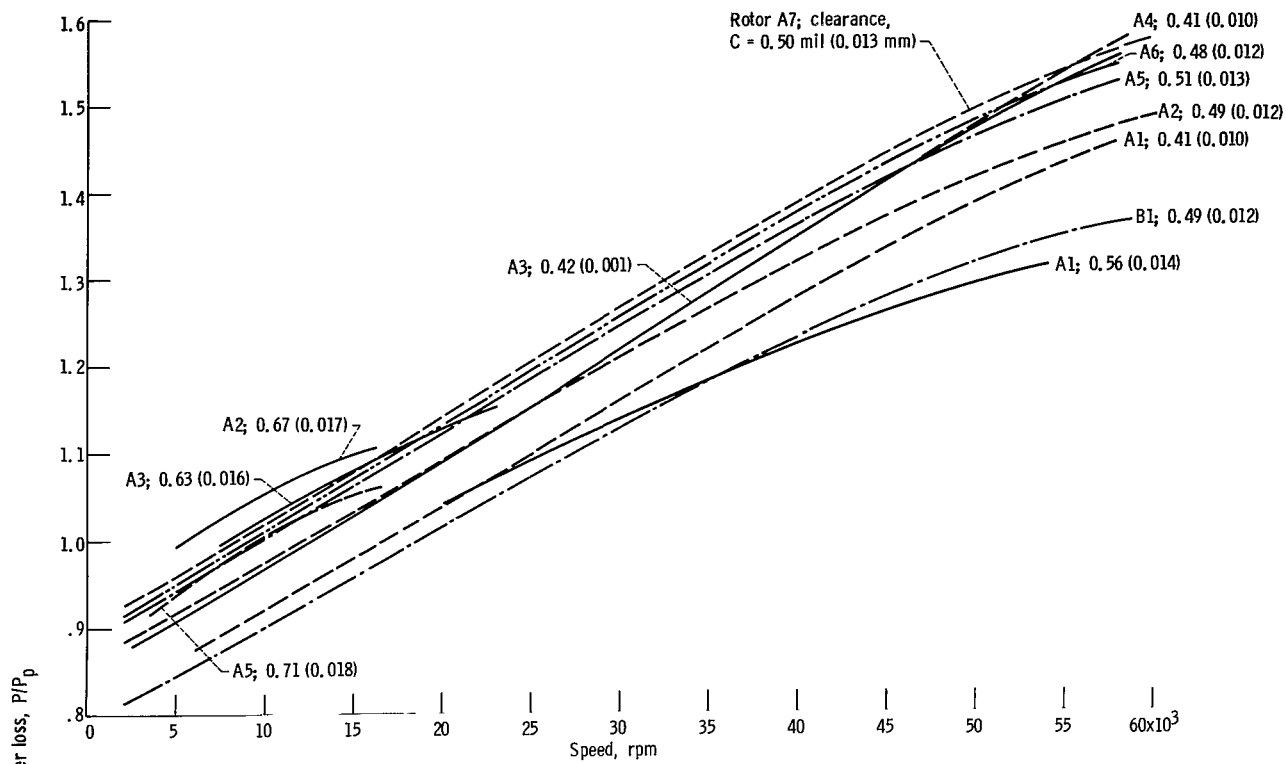
The most striking features of these figures are the close grouping of the curves and the fact that the relative power loss increases with speed at nearly the same rate for all of the configurations tested. The slope of the curves is approximately  $1.2 \times 10^{-5}$  per rpm. Several of the curves flatten out at high speed.

The parameter that is commonly used to characterize speed in gas lubrication work is the bearing number  $\Lambda$ .

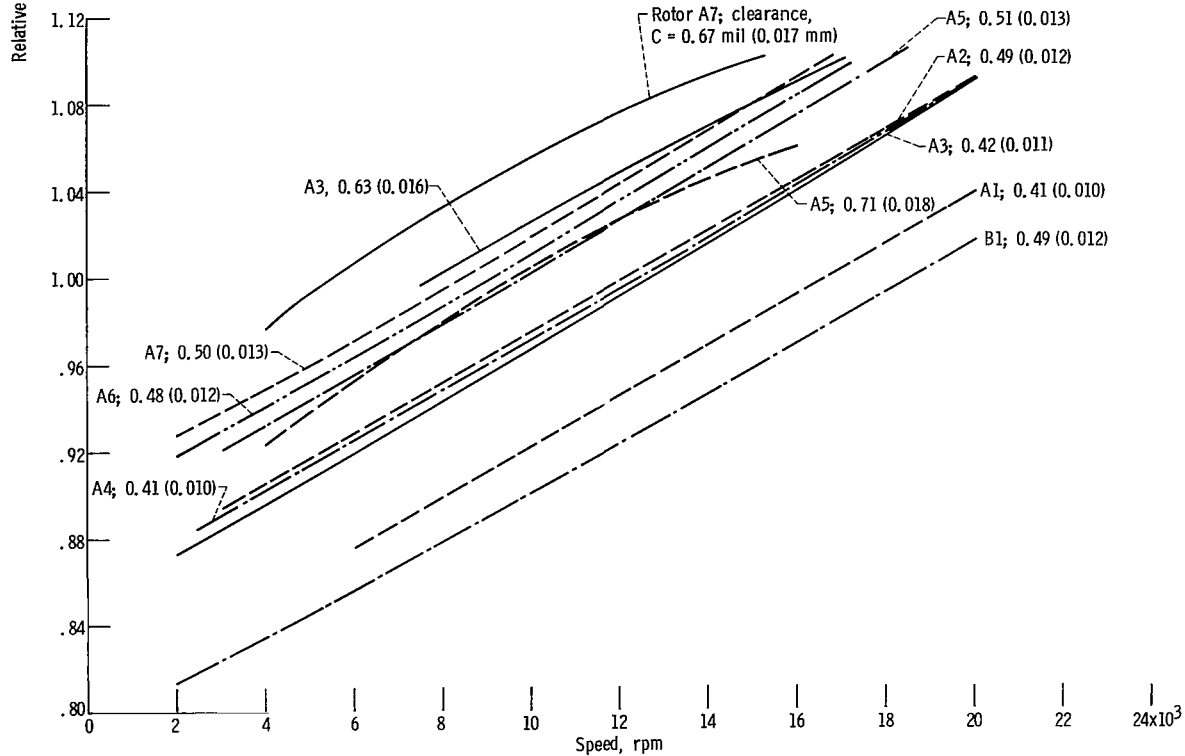
$$\Lambda = \frac{6\mu\omega}{p_a} \left(\frac{R}{C}\right)^2 \quad (13)$$

Figures 7(a) and (b) compare relative power losses among the various herringbone bearings tested using the bearing number as a speed parameter. Figure 7(a) shows the entire  $\Lambda$  range, and figure 7(b) the lower  $\Lambda$  values. The bearing number was calculated using the centrifugal growth corrected clearance. The curves are again grouped closely together, though not as closely as in figure 6. The leveling off of the curves at high speed is somewhat more pronounced than in figure 6, and the curves appear to radiate from a common point, rather than being parallel. There is a fairly consistent trend of higher relative power loss with increasing clearance. This trend can be explained by examination of the definition of  $\Lambda$  (eq. (13)). Since all of the factors appearing in  $\Lambda$ , except speed and clearance, remained constant throughout the work discussed herein, it follows that  $\Lambda$  is proportional to  $\text{rpm}/C^2$ . A larger clearance results in a lower value of  $\Lambda$  and a curve from figure 6 is shifted to the left when it is replotted in figure 7. All the curves have a positive slope, thus, moving a curve to the left will make it appear higher.

The positive slope of the curves of figures 6 and 7 can be explained as follows. The clearance in a herringbone-grooved bearing is conventionally expressed as the clearance over the ridges. In the grooves, the clearance is larger than this by the depth of the groove. The mean clearance is between these two values.



(a) All speeds.



(b) Lower speeds.

Figure 6. - Herringbone bearing power loss relative to plain journal bearing.

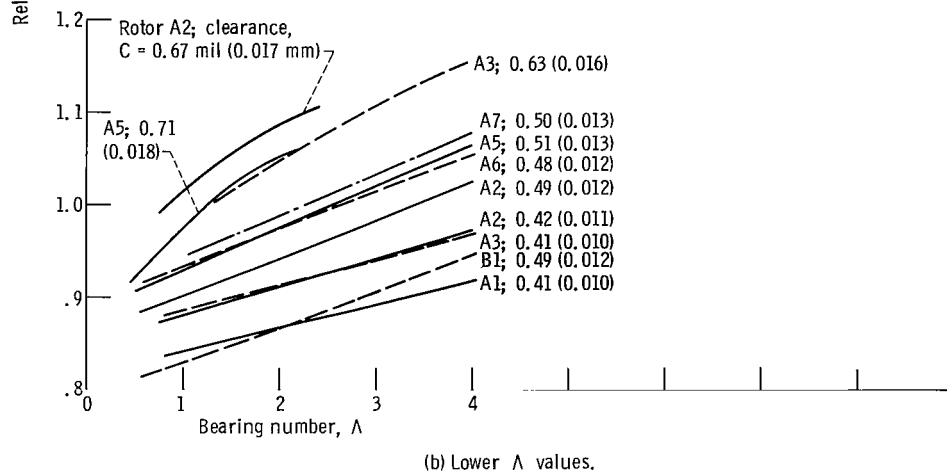
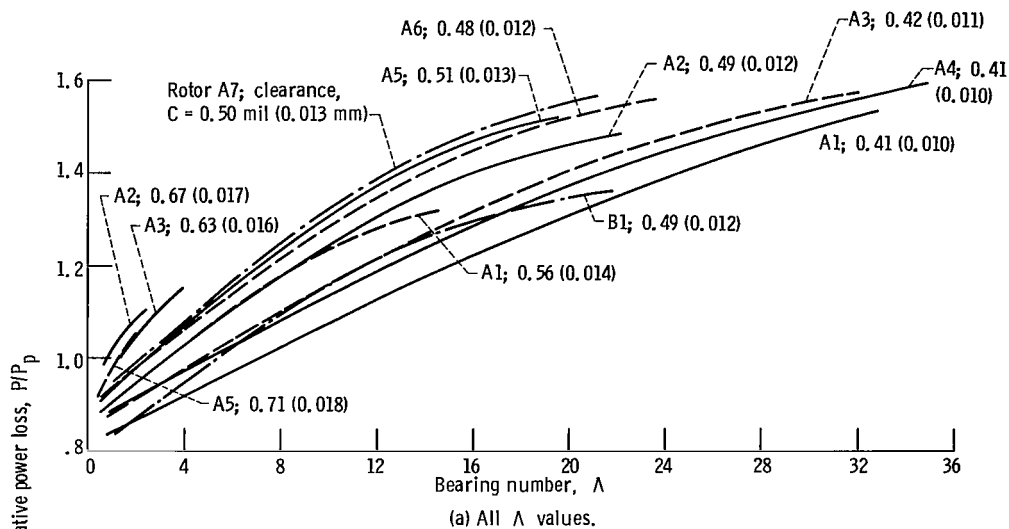


Figure 7. - Relative power loss versus bearing number.

At low speeds, the lubricant flow, due to rotation of the bearing, will be largely as given for the slow viscous flow at an inertialess fluid. This is illustrated by the plot of streamlines in figure 8(a). Under this condition, the average transverse velocity gradient in the groove is less than that over the ridges, and the power loss is less than that for a plain bearing whose clearance equals the ridge clearance.

As the speed increases, laminar eddies develop, and there is a circulation of fluid within the groove, approximately as depicted in figure 8(b). The effect of this circulation is to increase the power loss over that of the slow viscous flow case. It is reasonable to expect this increase to approach a limit as the laminar eddies become "fully developed"; this explains the leveling off of the curves of figures 6 and 7. True turbulence is not

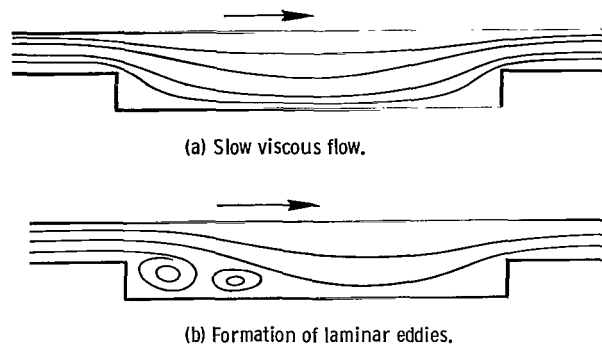


Figure 8. - Streamlines of flow in herringbone grooves.

expected to occur in gas-lubricated bearings since the Reynolds number based on clearance is far below the critical value for transition to turbulence (ref. 5). For example, when the groove clearance and maximum pressure in the bearing (calculated according to ref. 4) are used in the calculation of a Reynolds number, the largest attained in the experimental work was 440 for rotor  $B_1$  ( $C_o = 0.49$  mil;  $0.012$  mm). This is the maximum Reynolds number and is far below the transition (1730 for this configuration, ref. 5).

With this information on eddies and Reynolds number effects, it may be instructive to plot relative power loss using Reynolds number as a speed parameter. This has been done in figure 9. The density used in calculating the Reynolds number is that corresponding to the mean pressure in the grooved region of the bearing (ref. 4); the clearance is that over the ridges.

The correlation of the data is not noticeably better in figure 9 than in figures 6 and 7. All but two of the curves are within a fairly narrow band representing a range of power loss of about 12 percent at any one Reynolds number.

Some general observations can be made from figures 6, 7, and 9. The spread of the curves is fairly small in all the figures; the greatest is about 25 percent. The spread is least when the dimensional speed is used as the independent variable (fig. 6), rather than either of the dimensionless parameters (figs. 7 and 9). In figure 6 the variation among the curves at 50 000 rpm is only 15 percent. On all three figures, rotors A6 and A7, with narrower grooves than the others ( $\alpha = 0.3$  versus  $0.5$ ), show generally higher power loss. Among the other rotors, there appears to be a slight trend toward increasing power loss with increasing groove angle  $\beta$ . The depth of the grooves does not seem to affect power loss. The one fully grooved rotor (B1) seems to have a lower power loss than the other, partially grooved rotors. On the whole, differences among the various herringbone configurations are slight.

Perhaps the most widely used gas journal bearing in prototype turbomachinery is the tilting-pad bearing. If herringbone bearings are considered as replacements for tilting-pad bearings, knowledge of the respective power losses would be useful. Refer-

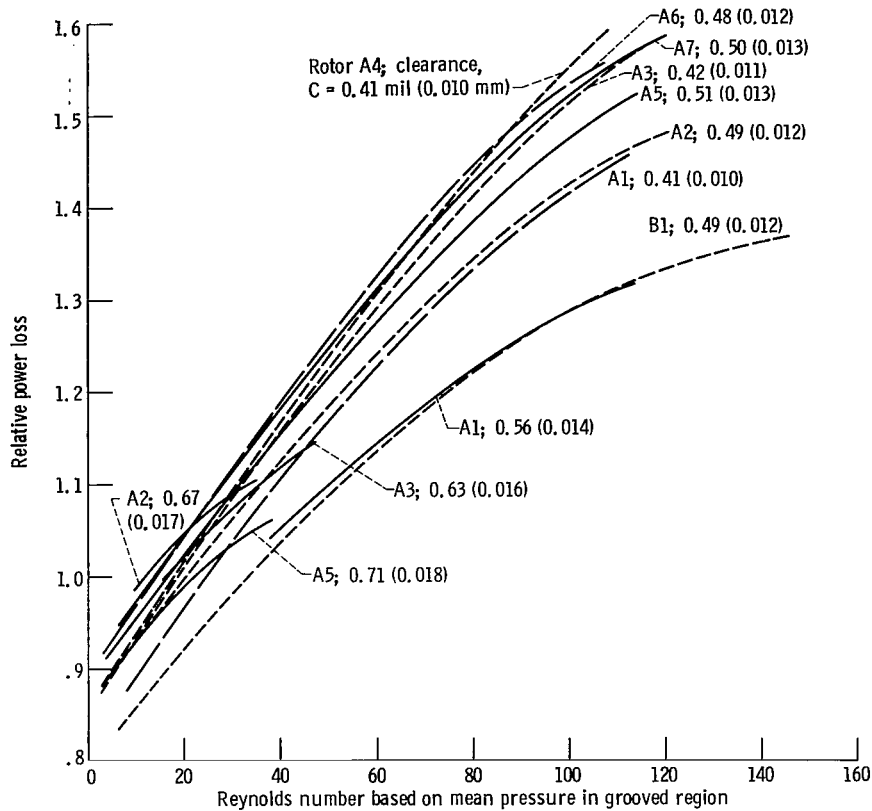


Figure 9. - Relative power loss versus Reynolds number.

ence 1 estimates the power loss for two three-pad journal bearings as 120 watts at 38 500 rpm. These bearings have a diameter of 1.75 inches (4.3 cm) and a length to diameter ratio of 0.75 (ref. 6). The lubricant gas was argon. The present test bearings have a diameter of 1.5 inches (3.8 cm), a length to diameter ratio of 1, and operate in air. In order to have a basis for comparison, it will be assumed that equation (11) applies to the tilting-pad bearing, except for a proportionality factor. It will be further assumed that, in reducing the size of the bearing, the ratio of radius to clearance remains constant. Then, for operation at constant speed,

$$P \propto \mu R^3 \frac{L}{D} \quad (15)$$

The power loss in two tilting-pad bearings operating in air and having the same dimensions as the present herringbone bearings would then be 83 watts (viscosity data taken from ref. 7). The power loss in the experimental herringbone bearing at 38 500 rpm varied from 89 to 138 watts; the average was 116 watts. Thus the herringbone-bearing

power loss is, on the average, 1.4 times that in the example tilting-pad bearing. Whether the advantages of the herringbone bearing (fewer parts, smaller bearing envelope, higher load capacity) compensate for the increased power loss must be evaluated for the particular application. Because of its increasing load capacity at higher speeds, it may be possible to use a smaller herringbone bearing than the tilting-pad bearing in a given application; therefore, it is possible that power loss could be reduced by using herringbone bearings.

## SUMMARY OF RESULTS

Experiments were conducted to determine the power loss in herringbone-grooved journal bearings operating in air to speeds of 60 000 rpm. The power loss was calculated from the speed-time plot of the bearing rotor coasting down in speed. The following results were obtained:

1. Within the range of geometric variables used, power loss (relative to that calculated for a plain bearing of the same dimensions) does not vary widely. Power loss appears to increase slightly with increasing groove angle and decreasing groove width. The one fully grooved rotor tested had generally lower power loss than the partially grooved rotors. Groove depth did not seem to influence power loss.

2. Relative power loss increases with speed. Except at low speeds, power loss was greater in the herringbone bearings than in equivalent size plain bearings. Power loss increased with speed at nearly the same rate in all the herringbone bearings used.

3. Dimensional power loss at 38 500 rpm was somewhat greater than that in a reference tilting-pad bearing.

4. Relative power loss was correlated best by using dimensional speed as the independent variable. At 50 000 rpm relative power loss varied by only 15 percent among the configurations tested. Correlations with bearing number  $\Lambda$  and Reynolds number were not as good.

Lewis Research Center,  
National Aeronautics and Space Administration,  
Cleveland, Ohio, February 7, 1969,  
129-03-13-05-22.

## REFERENCES

1. Wong, R. Y.; Stewart, W. L.; and Rohlik, H. E.: Pivoted-Pad Journal Gas Bearing Performance in Exploratory Operation in Brayton Cycle Turbocompressor. *J. Lubr. Tech.*, vol. 90, no. 4, Oct. 1968, pp. 687-696.
2. Cunningham, Robert E.; Fleming, David P.; and Anderson, William J.: Experiments on Stability of Herringbone-Grooved Gas-Lubricated Journal Bearings to High Compressibility Numbers. NASA TN D-4440, 1968.
3. Timoshenko, S.: *Theory of Elasticity*. McGraw-Hill Book Co., Inc., 1934, pp. 63 and 68.
4. Vohr, J. H.; and Chow, C. Y.: Characteristics of Herringbone-Grooved, Gas-Lubricated Journal Bearings. *J. Basic Eng.*, vol. 87, no. 3, Sept. 1965, pp. 568-578.
5. Taylor, G. I.: Stability of a Viscous Liquid contained between Two Rotating Cylinders. *Phil. Trans. Roy. Soc. London, ser. A*, vol. 223, 1923, pp. 289-343.
6. Anon.: Design and Fabrication of a High-Performance Brayton Cycle Radial-Flow Gas Generator. NASA CR-706, 1967.
7. Hodgman, Charles D., ed.: *Handbook of Chemistry and Physics*. 42nd ed., Chemical Rubber Publ. Co., 1961.

FIRST CLASS MAIL

POSTMASTER: If Undeliverable (Section 158  
Postal Manual) Do Not Return

*"The aeronautical and space activities of the United States shall be conducted so as to contribute . . . to the expansion of human knowledge of phenomena in the atmosphere and space. The Administration shall provide for the widest practicable and appropriate dissemination of information concerning its activities and the results thereof."*

— NATIONAL AERONAUTICS AND SPACE ACT OF 1958

## NASA SCIENTIFIC AND TECHNICAL PUBLICATIONS

**TECHNICAL REPORTS:** Scientific and technical information considered important, complete, and a lasting contribution to existing knowledge.

**TECHNICAL NOTES:** Information less broad in scope but nevertheless of importance as a contribution to existing knowledge.

**TECHNICAL MEMORANDUMS:** Information receiving limited distribution because of preliminary data, security classification, or other reasons.

**CONTRACTOR REPORTS:** Scientific and technical information generated under a NASA contract or grant and considered an important contribution to existing knowledge.

**TECHNICAL TRANSLATIONS:** Information published in a foreign language considered to merit NASA distribution in English.

**SPECIAL PUBLICATIONS:** Information derived from or of value to NASA activities. Publications include conference proceedings, monographs, data compilations, handbooks, sourcebooks, and special bibliographies.

**TECHNOLOGY UTILIZATION PUBLICATIONS:** Information on technology used by NASA that may be of particular interest in commercial and other non-aerospace applications. Publications include Tech Briefs, Technology Utilization Reports and Notes, and Technology Surveys.

*Details on the availability of these publications may be obtained from:*

**SCIENTIFIC AND TECHNICAL INFORMATION DIVISION  
NATIONAL AERONAUTICS AND SPACE ADMINISTRATION  
Washington, D.C. 20546**